J|A|C|S ARTICLES

Published on Web 09/10/2010

Multistep N_2 Breathing in the Metal−Organic Framework Co(1,4-benzenedipyrazolate)

Fabrice Salles,[†] Guillaume Maurin,*[,†] Christian Serre,[‡] Philip L. Llewellyn,[§] Christina Knöfel,[§] Hye Jin Choi,[||] Yaroslav Filinchuk,[⊥] Laetitia Oliviero,[#] Alexandre Vimont,[#] Jeffrey R. Long,*[,||] and Gérard Férey[‡]

Institut Charles Gerhardt Montpellier, UMR CNRS 5253, Université Montpellier 2, Place E. Bataillon, 34095 Montpellier Cedex 05, France, Institut Lavoisier, UMR CNRS 8180, Université de Versailles, Saint Quentin en Yvelines, 78035 Versailles Cedex, France, Laboratoire Chimie Provence, Universités d'Aix-Marseille I, II & III - CNRS, UMR 6264, Centre de Saint-Jérôme, 13397 Marseille, France, Department of Chemistry, University of California, Berkeley, California 94720, USA, SNBL at ESRF, B.P. 220, 38043 Grenoble Cedex, France, and Laboratoire Catalyse et Spectrochimie, ENISCAEN, Université de Caen, CNRS, 6 Bd Maréchal Juin, F-14050 Caen, France

Received May 19, 2010; E-mail: guillaume.maurin@univ-montp2.fr; jrlong@berkeley.edu

Abstract: A variety of spectroscopic techniques combined with *in situ* pressure-controlled X-ray diffraction and molecular simulations have been utilized to characterize the five-step phase transition observed upon N_2 adsorption within the high-surface area metal−organic framework Co(BDP) (BDP^{2-} = 1,4-benzenedipyrozolate). The computationally assisted structure determinations reveal structural changes involving the orientation of the benzene rings relative to the pyrazolate rings, the dihedral angles for the pyrazolate rings bound at the metal centers, and a change in the metal coordination geometry from square planar to tetrahedral. Variable-temperature magnetic susceptibility measurements and *in situ* infrared and UV−vis−NIR spectroscopic measurements provide strong corroborating evidence for the observed changes in structure. In addition, the results from *in situ* microcalorimetry measurements show that an additional heat of 2 kJ/mol is required for each of the first four transitions, while 7 kJ/mol is necessary for the last step involving the transformation of Co^{II} from square planar to tetrahedral. Based on the enthalpy, a weak N_2 interaction with the open Co^{II} coordination sites is proposed for the first four phases, which is supported by Monte Carlo simulations.

Introduction

Over the past decade, metal−organic frameworks have emerged as one of the most promising classes of microporous materials,[1] particularly in view of their potential applications in catalysis,[2] gas separation/storage,[3] and drug delivery.[4] Within this family, some solids exhibit great flexibility (the so-called 'breathing')[5] which can reach a variation in unit cell volume between the open and closed phases of greater than 300%.[6] Most of the time, the adsorption of gases by these swelling solids occurs via one of two mechanisms.[5,7] One pathway involves an evacuated open phase shrinking first and then expanding at higher pressure. Alternatively, the evacuated solid is closed and progressively opens as the pressure increases. Such a breathing effect, initially considered as a laboratory curiosity, is now extensively studied for both academic and industrial purposes.[5] The remarkable sensitivity of flexible solids to external stimuli can render them excellent candidates as sensors for the evaluation of adsorbent−adsorbate and adsorbate−adsorbate interactions.[8] More specifically, a framework material exhibiting different pore-opening pressures depending upon various gas species with a sharp adsorption saturation (a plateau) in its isotherm would perhaps increase the chance for applications in

[†] Université Montpellier 2.
[‡] Université de Versailles.
[§] Universités d'Aix-Marseille I, II, & III - CNRS.
[||] University of California.
[⊥] SNBL at ESRF.
[#] Université de Caen.

(1) (a) Eddaoudi, M.; Kim, J.; Rosi, N.; Vodak, D.; Wachter, J.; O'Keeffe, M.; Yaghi, O. M. *Science* **2002**, *295*, 469. (b) Kitagawa, S.; Kitaura, R.; Noro, S.-I. *Angew. Chem., Int. Ed.* **2004**, *43*, 2334. (c) Férey, G. *Chem. Soc. Rev.* **2008**, *37*, 191.
(2) (a) Ma, L.; Abney, C.; Lin, W. *Chem. Soc. Rev.* **2009**, *38*, 1248. (b) Lee, J.; Farha, O. K.; Roberts, J.; Scheidt, K. A.; Nguyen, S. T.; Hupp, J. T. *Chem. Soc. Rev.* **2009**, *38*, 1450.
(3) (a) Murray, L. J.; Dinca, M.; Long, J. R. *Chem. Soc. Rev.* **2009**, *38*, 1294. (b) Li, J.-R.; Kuppler, R. J.; Zhou, H.-C. *Chem. Soc. Rev.* **2009**, *38*, 1477. (c) Hamon, L.; Llewellyn, P. L.; Devic, T.; Ghoufi, A.; Clet, G.; Guillerm, V.; Pirngruber, G. D.; Maurin, G.; Serre, C.; Driver, G.; van Beek, W.; Jolimaitre, E.; Vimont, A.; Daturi, M.; Férey, G. *J. Am. Chem. Soc.* **2009**, *131*, 17490.
(4) (a) Taylor-Pashow, K. M. L.; Della Rocca, J.; Xie, Z. G.; Tran, S.; Lin, W. B. *J. Am. Chem. Soc.* **2009**, *131*, 14261. (b) Horcajada, P.; et al. *Nat. Mater.* **2010**, *9*, 172.
(5) Férey, G.; Serre, C. *Chem. Soc. Rev.* **2009**, *38*, 1380.
(6) Serre, C.; Mellot-Draznieks, C.; Surblé, S.; Audebrand, N.; Filinchuk, Y.; Férey, G. *Science* **2007**, *315*, 1828.
(7) (a) Serre, C.; Bourrelly, S.; Vimont, A.; Ramsahye, N.; Maurin, G.; Llewellyn, P. L.; Daturi, M.; Filinchuk, Y.; Leynaud, O.; Barnes, P.; Férey, G. *Adv. Mater.* **2007**, *19*, 2246. (b) Salles, F.; Ghoufi, A.; Maurin, G.; Bell, R. G.; Mellot-Draznieks, C.; Férey, G. *Angew. Chem., Int. Ed.* **2008**, *47*, 8487.
(8) Millange, F.; Serre, C.; Guillou, N.; Férey, G.; Walton, R. I. *Angew. Chem., Int. Ed.* **2008**, *47*, 4100.

 10.1021/ja104357r

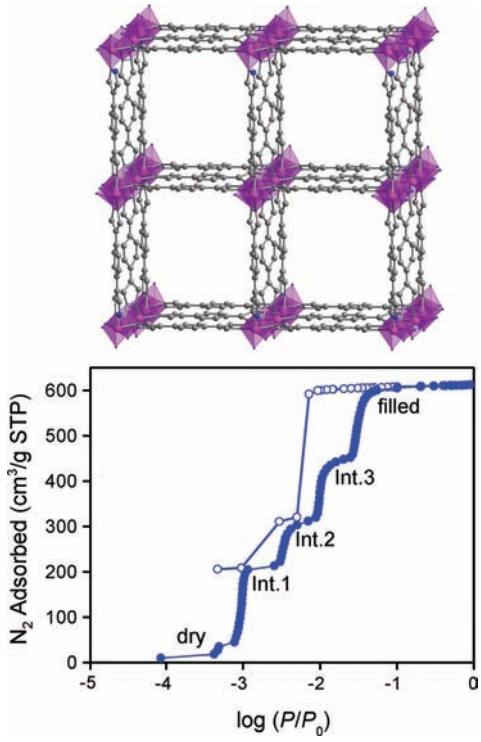

Figure 1. Pseudotetragonal unit cell of **1** (top), with purple, gray, and blue spheres representing Co, C, and N atoms, respectively; solvent molecules and H atoms are omitted for clarity. N_2 adsorption isotherm (bottom) measured at 77 K, indicating the five pressure-dependent phases. Filled and empty symbols represent adsorption and desorption, respectively.[10]

a pressure swing adsorption gas purification method.[9a] Indeed, a highly effective separation of CO_2 over CH_4 has recently been demonstrated for a flexible metal−organic framework.[9b]

Featuring a high surface area and a broad hysteresis for H_2 adsorption, Co(BDP) (BDP^{2-} = 1,4-benzenedipyrazolate; **1d**) represents a rare example of a metal−organic framework exhibiting flexibility upon adsorption of nonpolar molecules such as H_2 or N_2.[10] Moreover, the presence of five well-pronounced steps in its N_2 adsorption isotherm (see Figure 1) is without precedent and has piqued our curiosity as to the origins of the phase transitions. *In situ* synchrotron X-ray powder diffraction experiments performed on the compound under various N_2 pressures combined with appropriate computational tools have now enabled us to propose a complete structural analysis of each phase involved in the adsorption, as further supported experimentally by magnetic susceptibility and spectroscopic measurements. In addition, a weak binding of N_2 at the open Co^{II} sites of the framework will be discussed in relation to results from microcalorimetry measurements and Monte Carlo simulations.

Experimental Section

Synthesis and Activation of Co(BDP).[10] A borosilicate tube (1.2 cm o.d. × 15 cm length) was charged with $Co(CF_3SO_3)_2$ (120 mg, 0.34 mmol), H_2BDP (60 mg, 0.29 mmol), and 2.0 mL of *N*,*N*-diethylformamide (DEF). The reaction mixture was degassed by the freeze−pump−thaw method (5 cycles), and the tube was sealed under reduced pressure. The tube was then heated in an oil bath at 150 °C for 6 days to afford a purple microcrystalline solid. Upon cooling to room temperature, the tube was broken open in air and the solid was immediately collected by filtration. The resulting solid was washed with successive aliquots of DEF (5 × 10 mL) and dried under reduced pressure for 30 min to afford 0.13 g (95%) of Co(BDP)·2DEF·H_2O. The compound was stored under an atmosphere of DEF vapor. IR (solid, ATR): $\nu_{C=C}$ 1576, $\nu_{C=N}$ 1433, 1399, $\nu_{C=O}$ 1658 cm^{-1}. Anal. Calcd for $C_{22}H_{32}CoN_6O_3$: C, 54.21; H, 6.62; N, 17.24. Found: C, 54.18; H, 5.95; N, 17.05. A dry activated sample of Co(BDP) was obtained by heating Co(BDP)·2DEF·H_2O at 160 °C under dynamic vacuum until an outgas rate of less than 2 mTorr/min (0.27 Pa/min) was achieved (after ca. 2 days).

Evolution of the XRPD Pattern with Pressure. *In situ* synchrotron powder diffraction patterns were collected at the Swiss-Norwegian Beamlines of the ESRF using an MAR345 image plate detector and a monochromatic beam with a wavelength of 0.700 00 Å. The sample-to-detector distance (250 or 400 mm) and parameters of the detector were calibrated using NIST standard LaB_6. Two-dimensional diffraction images were integrated by Fit2D software. The patterns were indexed using the Dicvol software.[11] Le Bail fits were then performed with the Fullprof2k software package using its graphical interface Winplotr.[12,13] A gas dosing system[14] (see Figure S1) was used to admit gases at 1 mbar to 40 bar of pressure into a 0.5 mm quartz capillary filled with a sample and exposed to the X-ray beam. The sample was first outgassed at elevated temperatures using a turbopump (10^{-6} mbar). The temperature was set in the 80−500 K range by Oxford Cryostream 700+. A typical data set at one pressure point was collected during 60 s.

Computationally Assisted Structure Determinations. The structure of the solid in its dry state was first constructed from scratch in the space group *C*2/*c* using the cell parameters obtained via the successful indexing of the experimental X-ray powder diffraction pattern. Initially, the fractional coordinates of each atom of the Co(BDP) framework were guessed from those of the Fe-1,4-benzenedicarboxylate unit present in the anhydrous form of Fe(OH)(BDC) (BDC^{2-} = 1,4-benznedicarboxylate; MIL-53(Fe)).[8,15] Indeed, the latter structure is revealed from both cell parameters, volumes, and space group to be topologically similar to the dry form of the Co(BDP). This structural model was then energy-minimized by means of density functional theory (DFT) simulations, maintaining fixed the experimental cell parameters obtained at 100 K. These calculations were performed considering the PW91 GGA density functional and the double numerical basis set containing polarization functions on hydrogen atoms (DNP) available in the DMol^3 code, as already successfully used to describe the behavior of other metal−organic frameworks.[16] The partial charges of each atom of the framework were also extracted from these DFT calculations using the Mulliken charge partitioning method. Starting from this crystallographic model for the dry state, the structures of the other intermediates (Int.1, Int.2, and Int.3) were then derived from an energy minimization procedure using the classical universal force field (UFF)[17] and imposing the unit cell parameters determined experimentally for each phase detected under a nitrogen atmosphere at 100 K. This latter force field has been selected for its ability to successfully determine the structures of many

(9) (a) Yang, R. T. *Gas Separation by Adsorption Processes*; Imperial College Press: 1997; Vol. 1, pp 237−247. (b) Couck, S.; Denayer, J. F. M.; Baron, G. V.; Rémy, T.; Gascon, J.; Kapteijn, F. *J. Am. Chem. Soc.* **2009**, *131*, 6326.
(10) Choi, H. J.; Dinca, M.; Long, J. R. *J. Am. Chem. Soc.* **2008**, *130*, 7848.
(11) Boultif, A.; Loüer, D. *J. Appl. Crystallogr.* **1991**, *24*, 987.
(12) Rodriguez-Carjaval, J. *Collected Abstracts of Powder Diffraction Meeting*; Toulouse, France, 1990; p 127.
(13) Roisnel, T.; Rodriguez-Carjaval, J. In *Abstract of the 7th European Powder Diffraction Conference*; Barcelona, Spain, 2000; p 71.
(14) Llewellyn, P. L.; Horcajada, P.; Maurin, G.; Devic, T.; Rosenbach, N.; Bourrelly, S.; Serre, C.; Vincent, D.; Loera-Serna, S.; Filinchuk, Y.; Férey, G. *J. Am. Chem. Soc.* **2009**, *131*, 13002.
(15) Millange, F.; Guillou, N.; Walton, R. I.; Greneche, J. M.; Margiolaki, I.; Férey, G. *Chem. Commun.* **2008**, 4732.
(16) Rappé, K.; Casewit, C. J.; Colwell, K. S.; Goddard, W. A., III; Skiff, W. M. *J. Am. Chem. Soc.* **1992**, *114*, 10024.
(17) Ramsahye, N.; Maurin, G.; Bourrelly, S.; Llewellyn, P. L.; Serre, C.; Loiseau, T.; Devic, T.; Férey, G. *J. Phys. Chem. C* **2008**, *112*, 514.

metal−organic frameworks,[14,18,19,24b] including the structurally analogous phase MIL-53(Fe).[24b] Such calculations were performed using the Forcite software. The Ewald summation was employed to evaluate the electrostatic interactions. van der Waals interactions (represented by a classical 12-6 Lennard−Jones potential) beyond 12.5 Å were neglected. The convergence criteria were set to 1.0×10^{-4} kcal/mol (energy), 0.005 kcal/mol·Å (forces), and 5.0×10^{-5} Å (displacement), respectively. The resulting structures were then geometry-refined at the DFT level to finally provide a plausible crystal structure for each intermediate form whose powder XRPD patterns were further calculated using the Reflex software. For the filled form, we considered the structure previously reported from the single crystal X-ray analysis. The simulated powder diffraction patterns of the different forms of the Co(BDP) flexible metal−organic framework were compared to the experimental ones. Please note that peak widths have been defined for the simulated pattern using a fixed fwhm value (Powder cell Software), leading to some discrepancies in relative intensities due to the 2-θ dependence of the experimental peak width and the presence of peak broadening, particularly for the dry and the Int.1 phases. While the simulated powder diffraction patterns of the dry form match well the experimental ones (see Figure S2a), one should notice from Figure S2b to Figure S2d that the experimental patterns recorded for a given N_2 pressure indicate the coexistence of at least two structural forms, as evidenced by the simulated patterns.

Grand Canonical Monte Carlo Simulations. The absolute N_2 adsorption isotherms for the different structures were computed up to 1 bar at 77 K using Grand Canonical Monte Carlo (GCMC) simulations. The N_2 molecule was represented by a three-point charges model developed by Murthy et al.,[20] while the atoms of the framework were described by the UFF force field.[17] The N_2-framework interactions consisted of a repulsion−dispersion 12-6 Lennard−Jones (LJ) term and a Coulombic contribution. The corresponding LJ parameters were calculated using the mixing Lorentz−Berthelot combination rules. A simulation box of 8 ($2 \times 2 \times 2$ for the open form), 12 ($1 \times 3 \times 4$ for the Int.1 form), and 16 rigid unit cells ($1 \times 4 \times 4$ for the dry structure and $2 \times 2 \times 4$ for the Int.2 and Int.3 structures) with typically 2×10^6 Monte Carlo steps was considered in these calculations. Short-range interactions were estimated using a cutoff distance of 12 Å, and an Ewald summation was used to compute the electrostatic interactions.

Adsorption Microcalorimetry at 77 K. Prior to each adsorption experiment, the sample was outgassed using sample controlled thermal analysis (SCTA).[21] Here, the sample was heated under a constant residual vacuum pressure of 0.02 mbar up to the final temperature of 150 °C for 16 h. The differential adsorption enthalpies were obtained directly using a Tian-Calvet type microcalorimeter coupled to a manometric apparatus built in house.[22] Approximately 50 mg of sample was placed in the microcalorimeter which was immersed within a liquid nitrogen cryostat. A quasi-equilibrium system of gas introduction allowed the determination of the adsorption isotherms and the corresponding microcalorimetric characterization with a high resolution.

Magnetic Measurements. A sample of Co(BDP)·2(DEF)·H_2O (**1**) was prepared for magnetic measurements by adding 26.4 mg of microcrystals to a gel capsule with eicosane (52 mg) melted on top of it. The dried compound, Co(BDP) (**1d**), was prepared by washing **1** with anhydrous dichloromethane in a glovebag filled with N_2, followed by desolvation at 170 °C under dynamic vacuum. A sample of **1d** for magnetic measurements was prepared by adding 22.5 mg of microcrystals to a quartz tube (2.8 mm ×100 mm). After being evacuated, the tube was sealed using a hydrogen/oxygen flame. Variable-temperature dc magnetic susceptibility data were collected from 5 to 300 K at an applied field of 1 kOe using a Quantum Design MPMS2 SQUID magnetometer. All of the data were corrected for the diamagnetic background, including for the gel capsule, eicosane, and quartz tube, with Pascal's constants that give $\chi_{dia} = -0.0001748$ emu/mol and -0.0000346 emu/mol for **1** and **1d**, respectively. A pressurized sample (**1d-N_2**) was prepared for magnetic measurements by applying a pressure of N_2 (100 mmHg) to a sample of **1d** in a quartz tube at 77 K using a Micromeretics ASAP2000 gas sorption analyzer, followed by sealing at 77 K. Magnetic data of χT values for **1** and **1d** were fit to the Fischer equation (eq 1) that expresses the exchange coupling between paramagnetic centers in an infinite chain system.

$$\chi = \frac{Ng^2\beta^2 S(S+1)}{3kT}\frac{1+u}{1-u}$$
$$u = \coth\left[\frac{JS(S+1)}{kT}\right] - \left[\frac{kT}{JS(S+1)}\right] \quad (1)$$

Here, N, β, g, k, and J represent Avogadro's number, the Bohr magneton, the Lande g-factor, the Boltzmann constant, and the magnetic exchange coupling parameter, respectively. Plots of $\chi_M T$ versus T are depicted in Figure 5.

***In Situ* Infrared Spectroscopy.** The solid dispersed in DEF was deposited on a silicon wafer and then placed in a quartz infrared cell equipped with KBr windows. A movable quartz sample holder allowed the sample to be placed in the infrared beam for measurements or into the furnace for thermal treatment. The cell was connected to a vacuum line for evacuation, calcinations, and the introduction of doses of gas or solvent vapor. In the present study, the sample was activated at 423 K over the course of 1 h under secondary vacuum. In the acetonitrile adsorption experiments, spectra were recorded at room temperature. The integration of the ν(CN) bands allowed us to estimate the relative amounts of adsorbed acetonitrile. In the CO adsorption experiment, the temperature of the pellet was decreased to about 100 K by cooling the sample holder with liquid N_2 after quenching the sample from the thermal treatment temperature. The probe pressure inside the infrared cell was monitored by two pressure gauges ($1-10^3$ Pa and $1-10^4$ Pa range). Transmission spectra were recorded in the 500−5600 cm^{-1} range at 4 cm^{-1} resolution on a Nicolet Nexus spectrometer equipped with an extended KBr beam-splitting device and a mercury cadmium telluride (MCT) cryodetector.

***In Situ* UV−vis−NIR Spectroscopy.** The UV−vis−NIR spectra were measured *in situ* in a flow cell (Harrick, Inc.) equipped with a diffuse reflectance accessory. The UV−vis spectra (30 000−12 500 cm^{-1}) were recorded using a Cary 4000 spectrophotometer (Varian Corp.). The NIR spectra (12 500−4000 cm^{-1}) were recorded using a Nicolet 6700 spectrometer equipped with a white light source, a CaF_2 beam-splitting device, and an InGaAs detector. Spectra of **1** and **1d** were recorded at room temperature under a flow of dry argon gas. Compound **1d** was obtained after evacuation of DEF by heating compound **1** at 473 K under argon for 3 h.

Results and Discussion

Collection and Analysis of Powder X-ray Diffraction Data. The three-dimensional pseudotetragonal (space group $P222_1$) structure of the as-synthesized solid, Co(BDP)·2DEF·H_2O (DEF = *N*,*N*-diethylformamide; **1**), can be described as a 4^4 net composed of chains of tetrahedrally coordinated Co^{II} centers along [001] linked in the two orthogonal directions by bridging BDP^{2-} ligands (see Figure 1). The corresponding square channels along [001] are filled with DEF and water solvate molecules, which can be completely evacuated to generate **1d** by heating at 160 °C under vacuum. To probe the intriguing five-step isotherm, *in situ* powder X-ray diffraction studies were performed at 100 K using the Swiss-Norwegian Beamline at

(18) Surblé, S.; Serre, C.; Mellot-Draznieks, C.; Millange, F.; Férey, G. *Chem. Commun.* **2006**, 284.
(19) Sonnauer, A.; Hoffmann, F.; Froba, M.; Kienle, L.; Duppel, V.; Thommes, M.; Serre, C.; Férey, G.; Stock, N. *Angew. Chem., Int. Ed.* **2009**, *48*, 3849.
(20) Murthy, C. S.; Singer, K.; Klein, M. L.; Mc Donald, I. R. *Mol. Phys.* **1980**, *48*, 3849.
(21) Rouquerol, J. *Thermochim. Acta* **1989**, *144*, 209.
(22) Llewellyn, P. L.; Maurin, G. *C. R. Chim.* **2005**, *8*, 283.

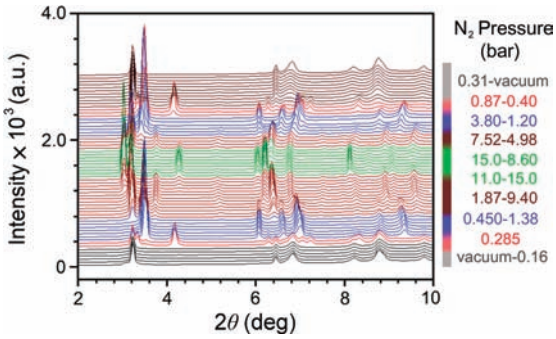

Figure 2. Layered plots of X-ray powder diffraction data measured at 100 K, where each pattern was measured under a constant N_2 pressure indicated as ranges. Note that the transition pressures are shifted with respect to those of the 77 K isotherm in Figure 1 owing to the increase of the saturation vapor pressure of N_2 upon warming.

Table 1. Unit Cell Parameters of Co(BDP) under a N_2 Atmosphere at 100 K[a]

phase	space group	*a* (Å)	*b* (Å)	*c* (Å)	*β* (deg)	*V* (Å³)
Dry	*C*2/*c*	24.87(5)	6.04(2)	7.22(2)	92.8(2)	1084
Int.1	*C*2/*c*	24.10(4)	10.48(2)	13.90(2)	94.1(1)	2 × 1754
Int.2	*C*2/*c*	23.17(2)	13.20(1)	6.98(1)	96.2(1)	2123
Int.3	*C*2/*c*	21.61(2)	15.55(1)	7.02(1)	97.7(1)	2338
Filled	$P4_122$	13.29(1)	13.29(1)	14.82(1)		2618

[a] As deduced from Dicvolgv through the graphical interface Winplotr[11] and further refined (via pattern matching) using Fullprof.[12]

the European Synchrotron Radiation Facility equipped with a custom-built apparatus to control the N_2 pressure above the sample.[23] As shown in Figure 2, sequential measurements of the powder X-ray diffraction pattern upon sweeping the N_2 pressure provided a remarkable phase evolution. Notably, the phase transitions occurred reversibly, reflecting the feasibility of repeated pore-opening and pore-closing cycles. Each distinct phase was scrutinized by collecting a diffraction pattern with a longer exposure time at a precise pressure and performing a unit cell indexing. The resulting cell parameters for the successive phases, denoted dry, Int.1, Int.2, Int.3, and filled, indicated a monoclinic cell with space group *C*2/*c* for the first four phases and revealed a remarkable shrinking of the cell volumes upon loss of guest molecules (see Table 1).

A computational strategy based on energy optimization techniques has proven highly effective in assisting with the difficult and time-consuming task of structure determination from powder X-ray diffraction data.[24] An analogous framework, MIL-53(Fe),[8,15] served as a starting point for identifying the structure of each phase of Co(BDP).[10] As a result of the X-ray analysis of **1d** coupled with the molecular simulations, a remarkable phase evolution was discovered, which indeed is associated with the change in coordination geometry at the Co^{II} centers (see Figure 3). Notably, the topology and symmetry of the framework in the monoclinic cells remain unaltered from dry to Int.3, demonstrating that Co^{II} adopts a square planar coordination geometry in all phases except filled, wherein it suddenly transforms to a tetrahedral geometry. Since this change is associated with a 90° rotation of two nitrogen atoms out of four while bridging Co^{II} chains, it causes a substantial reorientation of the ligands, although the simulated Co−N bond distances remain unchanged (mean Co−N = 1.955 Å) (see Figures S5 and S6).

The dihedral angle between pyrazolate rings (denoted α in Figure 3) estimated from the simulated structures corresponds to the large angle of the rhomb defining the channels within the monoclinic frameworks. With the progression of the pore-opening, α changes by decreasing from 152° to 108° for dry to Int.3, respectively. Also, the angle between two neighboring CoN_4 square planes along a chain increases from 133° in dry to 146° in Int.3 by increments, reflecting the transformation toward parallel alignment. In addition, a reorientation of the benzene rings is accompanied by every transition, which contributes to the small changes in the powder X-ray diffraction patterns (see Figure S2). Indeed, *in situ* infrared spectra for Co(BDP) recorded at 100 K confirmed that the C−N stretching vibrations for the pyrazolate rings have undergone transitions from dry to Int.1 and Int.1 to Int.2 upon increasing the N_2 pressure to 0.01 and 0.023 bar, respectively (see Figure 4, right). Since α turns strictly to 90° with the pair of pyrazolates aligned parallel in the filled phase, a pseudotetragonal symmetry is defined.

In terms of topology, the four monoclinic phases (dry−Int.3) are closely related to the MIL-53(Fe) structure type.[8,25] In a previous paper,[8] we showed that the evolution of the unit cell volume (*V*) in this class of materials can be analytically described as a function of the two diagonals of the lozenge (*d* and *D*, corresponding here to the unit cell parameters *b* and *a*, respectively):

$$V = k \sin[2 \arctan(d/D)] \qquad (2)$$

Indeed, the observed volumes of the different structures of Co(BDP) fit perfectly with the theoretical curve (see Figure S4). Accordingly, the four steps involving dry to Int.3 correspond to displacive transitions upon pore opening, whereas the last step to form the filled phase is a reconstructive transition (see Figures S5 and S6).

***In Situ* UV−vis−NIR and IR Spectra.** The expected geometry change at the Co^{II} centers in Co(BDP) during breathing is accompanied experimentally by a color change between purple for the dry phase and pink for the filled phase. UV−vis−NIR diffuse reflectance spectra recorded at room temperature for **1** and **1d** are shown at the left in Figure 4 and confirm the conversion from a tetrahedral to a square planar geometry for the Co^{II} centers upon desolvation through the disappearance of the shoulder at 10 500 cm^{-1} in the $^4A_2 \rightarrow {}^4T_1$ transition manifold.[26] Analogous color changes arise upon cooling a sample of **1d** under a N_2 atmosphere. A quartz tube containing **1d** was cooled to 77 K, filled with 0.13 bar of N_2, and sealed. Upon immersion of the tube in liquid nitrogen, the color of the solid was observed to change from purple to pink and then back to purple upon warming (see Figure S7).

Magnetic Susceptibility Data. Magnetic susceptibility measurements were performed on **1** and **1d** in anticipation of observing the differences between the Co^{II} centers adopting a high-spin ($S = {}^3/_2$) tetrahedral geometry in **1** versus a low-spin ($S = {}^1/_2$) square planar geometry in **1d**. As depicted in Figure 5, compound **1** displays a $\chi_M T$ value of 1.96 emu·K/mol at 300 K, near the spin-only value of 1.875 emu·K/mol expected for

(23) Llewellyn, P. L.; Horcajada, P.; Maurin, G.; Devic, T.; Rosenbach, N.; Bourrelly, S.; Serre, C.; Vincent, D.; Loera-Serna, S.; Filinchuk, Y.; Férey, G. *J. Am. Chem. Soc.* **2009**, *131*, 13002.
(24) (a) Mellot-Draznieks, C. *J. Mater. Chem.* **2007**, *17*, 4348. (b) Devic, T.; et al. *J. Am. Chem. Soc.* **2010**, *132*, 1127.
(25) Serre, C.; Millange, F.; Thouvenot, C.; Noguès, M.; Marsolier, G.; Loüer, D.; Férey, G. *J. Am. Chem. Soc.* **2002**, *124*, 13519.
(26) Everett, G. W., Jr.; Holm, R. H. *J. Am. Chem. Soc.* **1966**, *88*, 2442.

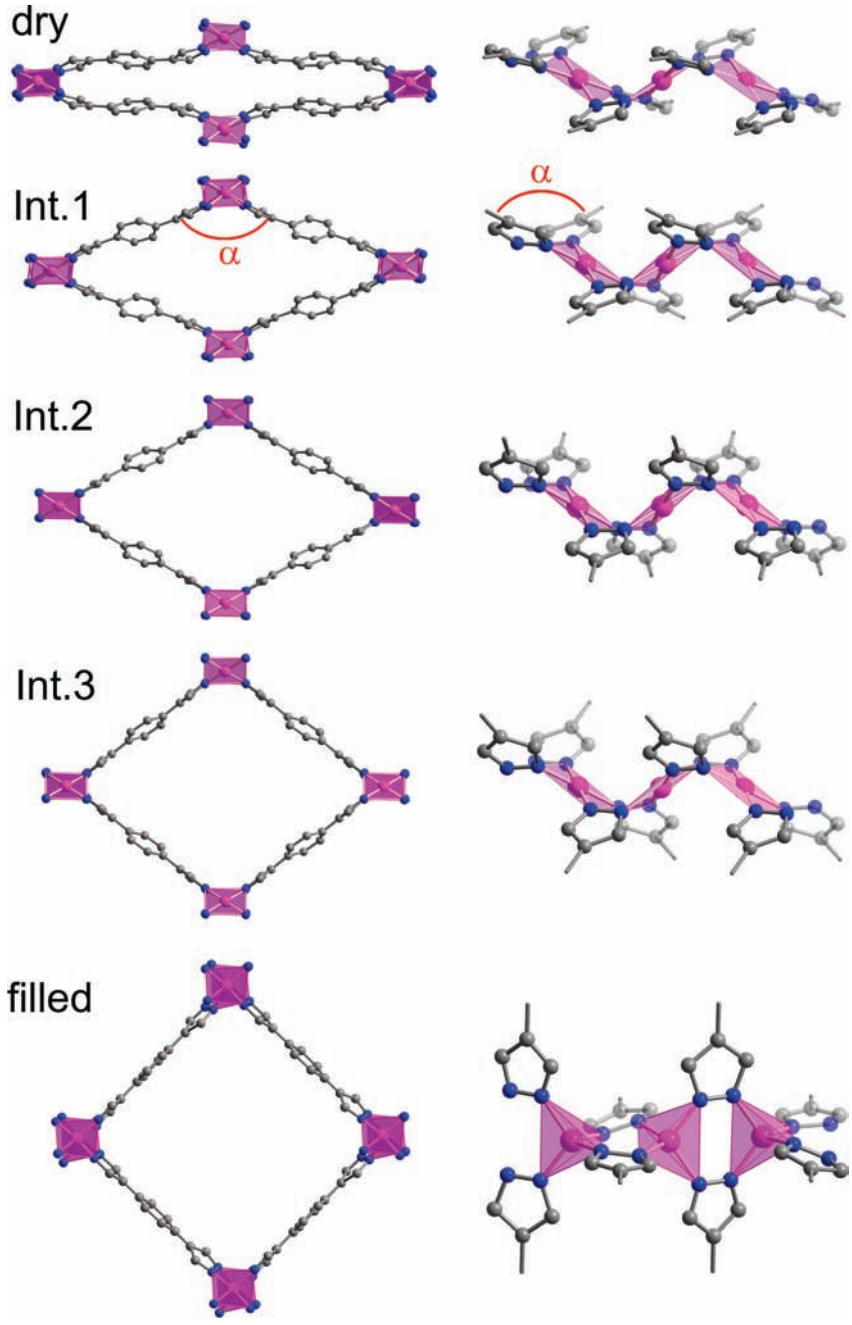

Figure 3. Simulated structures of Co(BDP), representing pressure-dependent pore evolution via five-step phase transition. The view down a single channel (left) and a portion of the Co^{II} chain (right) are shown for each structure with Co, N, and C atoms depicted as pink, blue, and gray spheres, respectively. Pressure ranges in which each phase was observed are vacuum, 0.2−0.25 bar, 0.45−0.55 bar, 1.9−3.2 bar, and 7.0−9.5 bar for dry, Int.1, Int.2, Int.3, and filled, respectively. Note that the monoclinic unit cell angle α for dry to Int.3 corresponds to the dihedral angle between two pyrazolate rings.

isolated metal centers with $S = {}^3/_2$. Upon cooling, the value of $\chi_M T$ drops steadily to near zero at 2 K, suggesting the presence of an antiferromagnetic exchange coupling between neighboring Co^{II} centers along the pyrazolate-bridged chains. Accordingly, the data were fit using Fisher's equation, which expresses the exchange coupling between paramagnetic centers linked in an infinite chain.[27] The best fit resulted in an exchange constant of $J = -9.2$ cm^{-1} and $g = 2.130$, in agreement with previous reports of antiferromagnetic exchange in pyrazolate- or tetrazolate-bridged Co^{II} compounds.[28] In contrast, **1d** exhibits a much lower magnetic moment at 300 K, with the value of $\chi_M T = 0.848$ emu·K/mol indicating an $S = {}^1/_2$ ground state with a g value significantly higher than 2.00. Such a large g value is in fact typical for low-spin Co^{II}, as assessed for various four- and five-coordinate complexes via EPR spectroscopy.[29] Indeed, the result is in good agreement with the square planar geometry

(27) Kahn, O. *Molecular Magnetism*; VCH: New York, 1993; pp 257−263.

(28) (a) Ehlert, M. K.; Rettig, S. J.; Storr, A.; Thompson, R. C.; Tortter, J. *Can. J. Chem.* **1993**, *71*, 1425. (b) Ouellette, W.; Prosvirin, A. V.; Whitenack, K.; Dunbar, K. R.; Zubieta, J. *Angew. Chem., Int. Ed.* **2009**, *48*, 2140.

(29) (a) Nishida, Y.; Kida, S. *Coord. Chem. Rev.* **1979**, *27*, 275, and references therein. (b) Jenkins, D. M.; Di Bilio, A. J.; Allen, M. J.; Betley, T. A.; Peters, J. C. *J. Am. Chem. Soc.* **2002**, *124*, 15336.

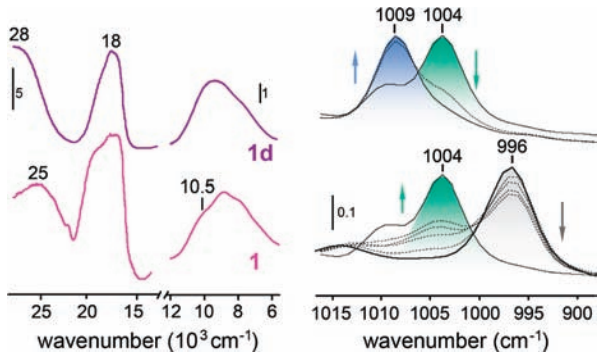

Figure 4. Left: UV−vis−NIR diffuse reflectance spectra for **1** (pink) and **1d** (purple). Right: Overlaid *in situ* infrared spectra for pyrazolate ring stretch vibrations in Co(BDP), as recorded at 100 K with increasing N_2 pressure up to 0.01 bar (lower) and from 0.01 to 0.023 bar (upper). These transitions are coincident with the phase transitions from dry (gray) to Int.1 (green) and from Int.1 to Int.2 (blue).

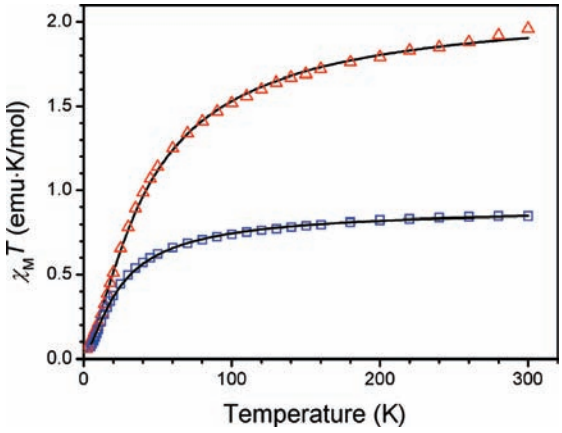

Figure 5. Temperature-variable magnetic susceptibility for **1** (△) and **1d** (□) measured at 1000 Oe and 2−300 K, along with the fit curves represented in solid lines (see the text for details).

predicted by computationally assisted structure determination. Here again, the value of $\chi_M T$ is seen to drop with decreasing temperature, indicating antiferromagnetic exchange coupling along the Co^{II} chains. Fitting the data using Fisher's equation resulted in $J = -26$ cm^{-1} and $g = 3.098$.

Microcalorimetry Measurements and Monte Carlo Simulations. As an additional probe of the phase changes, the enthalpy of N_2 adsorption was measured at 77 K employing an *in situ* pressure-controlled microcalorimeter. As shown in Figure 6, the five phases are distinctly differentiated with the enthalpy values of each step estimated as −14.7, −12.0, −9.5, −10.0, and −10.5 kJ/mol for dry, Int.1, Int.2, Int.3, and filled, respectively. The result is obviously distinguishable from a typical plot of an enthalpy of adsorption for a rigid microporous material, such as a zeolite.[18] The low-coverage enthalpy of −14.7 kJ/mol with its subsequent drop is presumably attributed to a weak N_2 binding at open Co^{II} coordination sites and is somewhat smaller in magnitude than those reported for zeolites (−19 to −27 kJ/mol).[30] Notably, significant valleys appear between each step, which is indicative of additional heat required for the phase transition concomitant with adsorption. While that energy is

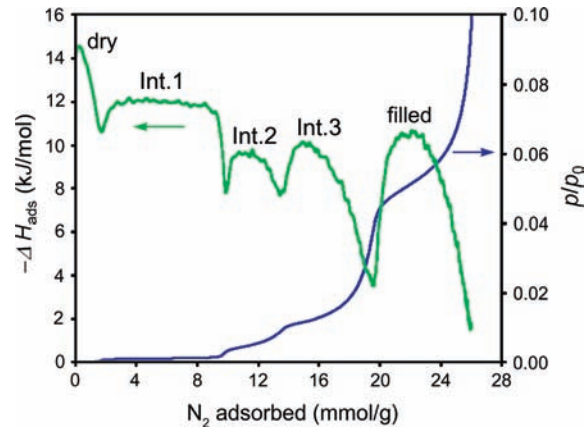

Figure 6. Enthalpy of N_2 adsorption measured at 77 K (green) in the low pressure range superimposed with the adsorption isotherm (blue).

estimated as ca. 2 kJ/mol for the dry through Int.3 transitions, it significantly increases to 7 kJ/mol for the last transition, reflecting the higher activation barrier associated with the transformation of the Co^{II} coordination geometry from square planar to tetrahedral. To the best of our knowledge, this is the first time such a complex transformation involving significant enthalpy changes has been measured directly during a gas adsorption at low temperature. Less complex behavior arose for CH_4 adsorption in **1d**, where only two steps were observed. Interestingly, four-step transitions from dry to Int.3 were also apparent in the infrared spectra of **1d** exposed to various CO pressures at 100 K (see Figure S8). Moreover, adsorption of acetonitrile below 0.013 bar at room temperature revealed a two-step isotherm characterized as the dry and Int.2 phases by infrared spectroscopy, with no evidence for the intervening Int.1 phase (see Figure S9). Thus, occurrence of the guest-dependent phase transitions appears to be associated with both the binding ability and size of the adsorbate molecule.

Monte Carlo simulations were undertaken in an attempt to identify the locations of the N_2 binding sites at 77 K for each form of Co(BDP). Adsorption of just one N_2 molecule per formula unit was found for the dry structure, wherein the adsorbate binds a Co^{II} center in a side-on fashion with a Co···N contact of 2.6 Å. This is a longer distance than typically observed for dinitrogen coordination complexes, indicating a rather weak interaction with N_2.[31] At higher loadings, the larger pore size results in N_2 molecules that are even further from the metal sites, with Co···N contacts falling in the range 3.2−3.4 Å for phases Int.1 through Int.3 (see Figures S10 and S11). Notably, N_2 molecules are primarily located near the open Co^{II} coordination sites in all of the phases except for the filled structure, for which an open site no longer exists. Overall, the saturation capacity for N_2 in each structure predicted from the Grand Canonical Monte Carlo simulations is in good agreement with that estimated from the measured isotherm, except for the filled phase where the full capacity was somewhat underestimated (see Figure S12).

Outlook

The aforementioned results provide the first in-depth study of the structural and thermodynamic origins of an unprecedented sequence of five phase transitions during N_2 adsorption in a

(30) Sebastian, J.; Vir Jasra, R. *Ind. Eng. Chem. Res.* **2005**, *44*, 8014, and references therein.

(31) Fryzuk, M. D. *Coord. Chem. Rev.* **2000**, *200*, 379.

flexible porous framework. This remarkable multistep breathing behavior, which is supported by a variety of *in situ* spectroscopic techniques, can be attributed to a combination of structural changes involving the orientation of the benzene rings relative to the pyrazolate rings, the dihedral angles for the pyrazolate rings bound at the metal centers, and a change in the metal coordination geometry from square planar to tetrahedral. In future work, an understanding of the nature of the phase transitions induced within Co(BDP) by various other adsorbates will be the focus, with an eye toward the development of potential applications in selective gas adsorption and molecular sensing.

Acknowledgment. This research was supported in the U.S. by the Department of Energy under Contract No. DE-AC02-05CH11231 and in France by ANR 'SAFHS' (ANR-07-BLAN-0284-02), 'NOMAC' (ANR-06-CO2-008), and the Region Lower-Normandy. We acknowledge the Swiss-Norwegian Beamlines for the in-house beamtime allocation and H. Leclerc for experimental assistance.

Supporting Information Available: Complete experimental details and refs 4b and 24b. This material is available free of charge via the Internet at http://pubs.acs.org.

JA104357R